Reactivities and Structural and Electrochemical Studies of Coordinatively Unsaturated Arene(dithiolato)Ru(II) Complexes [(η^6-*p*-cymene)Ru(1,2-$S_2C_2B_{10}H_{10}$-*S,S′*)] and [(η^6-C_6Me_6)Ru(1,2-$S_2C_2B_{10}H_{10}$-*S,S′*)]

Je-Hong Won,[†] Hong-Gyu Lim,[†] Bo Young Kim,[‡] Jong-Dae Lee,[†] Chongmok Lee,*[,‡] Young-Joo Lee,[†] Sungil Cho,[§] Jaejung Ko,*[,†] and Sang Ook Kang*[,†]

Department of Chemistry, Korea University, 208 Seochang, Chochiwon, Chung-nam 339-700, Korea, Department of Chemistry, Ewha Womans University, Seoul 120-750, Korea, and Department of Chemical Engineering, Junnong-dong 90, Seoul City University, Seoul 130-743, Korea

Received April 2, 2002

The addition reactions of 16-electron complexes [(η^6-arene)Ru(Cab$^{S,S'}$)] [**3**: arene = *p*-cymene (**3a**), C_6Me_6 (**3b**); Cab$^{S,S'}$ = 1,2-$S_2C_2B_{10}H_{10}$-*S,S′*] with the nucleophiles PEt_3, $CNBu^t$, and CO lead to the formation of the corresponding 18-electron complexes **4**−**6** [(η^6-arene)-Ru(Cab$^{S,S'}$)(L)] (L = PEt_3, $CNBu^t$, CO), which have been characterized by X-ray crystallography. Investigation of the redox process in a series of these base-adduct metalladithiolene complexes by cyclic voltammetry reveals a large dependence of the redox potentials on the nature of the ancillary η^6-arene and incoming L ligand. In an analogous manner, the reactivity of **3a** toward arylamines (**7**) has been found to produce [(η^6-*p*-cymene)Ru(Cab$^{S,S'}$)-(L)] (**8**) [L = η^1-$NH_2(CH_2CH_2)$Ar, Ar = C_6H_5 (**8a**); C_6H_4OMe (**8b**); $C_6H_3(OMe)_2$ (**8c**); C_8H_6N (**8d**)], having molecular structures closely related to those of **4** and **5**, as deduced by an electrochemical analysis and NMR studies. In addition, complex **3** reacts with a variety of substrates such as alkynes and a diazoalkane, generating a new class of dithiolato ruthenium-(II) complexes incorporating alkene and alkylidene units. Thus, the syntheses of the half-sandwich ruthenium(II) complexes [(η^6-arene)Ru{η^3-(*S,S,C′*)-$SC_2B_{10}H_{10}SC'R_2$}] [$C'R_2$ = (COOMe)C=C(COOMe) (**9**: arene = *p*-cymene (**9a**), C_6Me_6 (**9b**)), HC=CPh (**10**: arene = C_6Me_6 (**10b**)), CH_2SiMe_3 (**11**: arene = *p*-cymene (**11a**), C_6Me_6 (**11b**))] are reported, and the structure of **11b** has been established by an X-ray diffraction study. The formation of **9** and **10** has also been electrochemically investigated.

Introduction

We have recently reported the new coordination modes for the coordinatively unsaturated half-sandwich metal complexes[1] possessing an ancillary dithio-*o*-carboranyl ligand,[2] where the redox stability of the complexes showed a dependence on the ancillary ligand Cp or Cp*. For example, (η^5-Cp)Co(Cab$^{S,S'}$) (**I**) reacts with BH_3·THF to give a dinuclear complex of [(η^5-$CpCo)_2$-(Cab$^{S,S'}$)], while (η^5-Cp*)Co(Cab$^{S,S'}$) (**II**) was suppressed from making the dinuclear complex.[3] During the course of our previous work, we also found that the 16-electron complexes showed a reversible 0/−1 reduction with much less reversible 0/+1 oxidation, and the reversibility of the 0/+1 oxidation improved upon the addition of a donor ligand, i.e., the 18-electron complex. Consequently, the Cp* complex **II** displayed the enhanced reversibility of the 0/+1 oxidation compared with that of the Cp complex **I**. The differences shown in these reactions have stimulated our interest to investigate this area since they stem from the small difference in the ligand, i.e., Cp vs Cp* as shown in Chart 1.

Electrochemistry is the best method to monitor oxidation and reduction reactions.[4] However, not many studies have been done on the electrochemical behavior accompanying *o*-carboranyl complexes, especially those involving the *o*-carboranyl dithiolate. Therefore, we hope to develop and generalize this electrochemical methodology for the product analysis of *o*-carboranyl dithiolates. In the present study, we synthesized the (η^6-*p*-cymene)-

[†] Korea University.
[‡] Ewha Womans University.
[§] Seoul City University.

(1) (a) Ko, J.; Kang, S. O. *Adv. Organomet. Chem*. **2001**, *47*, 61. (b) Bae, J.-Y.; Lee, Y.-J.; Kim, S.-J.; Ko, J.; Cho, S.; Kang, S. O. *Organometallics* **2000**, *19*, 1514. (c) Kim, D.-H.; Ko, J.; Park, K.; Cho, S.; Kang, S. O. *Organometallics* **1999**, *18*, 2738. (d) Bae, J.-Y.; Park, Y.-I.; Ko, J.; Park, K.-I.; Cho, S.-I.; Kang, S. O. *Inorg. Chim. Acta* **1999**, *289*, 141.

(2) (a) Base, K.; Grinstaff, M. W. *Inorg. Chem*. **1998**, *37*, 1432. (b) Crespo, O.; Gimeno, M. C.; Jones, P. G.; Laguna, A. *J. Chem. Soc., Dalton Trans*. **1997**, 1099. (c) Crespo, O.; Gimeno, M. C.; Jones, P. G.; Laguna, A. *J. Chem. Soc., Chem. Commun*. **1993**, 1696. (d) Contreras, J. G.; Silva-trivino, L. M.; Solis, M. E. *J. Coord. Chem*. **1986**, *14*, 309. (e) Smith, H. D., Jr.; Robinson, M. A.; Papetti, S. *Inorg. Chem*. **1967**, *6*, 1014. (f) Smith, H. D., Jr.; Obenland, C. O.; Papetti, S. *Inorg. Chem*. **1966**, *5*, 1013. (g) Smith, H. D., Jr. *J. Am. Chem. Soc*. **1965**, *87*, 1817.

(3) Won, J.-H.; Kim, D.-H.; Kim, B. Y.; Kim, S.-J.; Lee, C.; Cho, S.; Ko, J.; Kang, S. O. *Organometallics* **2002**, *21*, 1443.

(4) Review: (a) Geiger, W. E. *Acc. Chem. Res*. **1995**, *28*, 351. (b) Tyler, D. R. *Acc. Chem. Res*. **1991**, *24*, 325. (c) Connelly, N. G. *Chem. Soc. Rev*. **1989**, *18*, 153. (d) Astruc, D. *Chem. Rev*. **1988**, *88*, 1189.

10.1021/om020259l CCC: $22.00
Publication on Web 11/23/2002

Chart 1

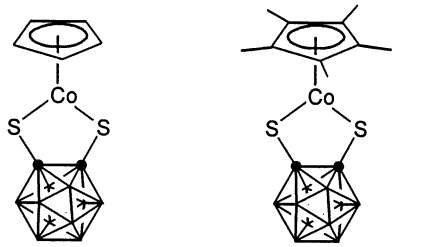

[(η^5-Cp)Co(Cab$^{S,S'}$)] **I** [(η^5-Cp*)Co(Cab$^{S,S'}$)] **II**

Chart 2

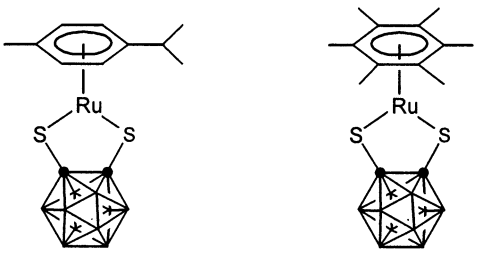

[(η^6-*p*-cymene)Ru(Cab$^{S,S'}$)] **3a** [(η^6-Me$_6$C$_6$)Ru(Cab$^{S,S'}$)] **3b**

Scheme 1. Synthesis of 16-Electron Metal Complexes 3[a]

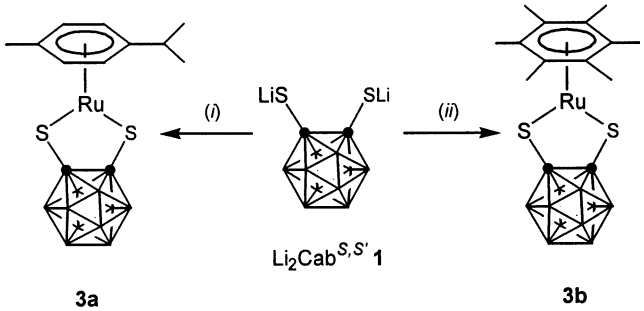

[a] (i) 1/2 [(*p*-cymeme)Ru(μ-Cl)Cl$_2$]$_2$ **2a**, THF, 0 °C; (ii) 1/2 [(C$_6$Me$_6$)Ru(μ-Cl)Cl]$_2$ **2b**, THF, 0 °C.

Ru(Cab$^{S,S'}$) (**3a**) and (η^6-C$_6$Me$_6$)Ru(Cab$^{S,S'}$) (**3b**) complexes and explored the chemistry of these complexes in terms of coordination chemistry and redox chemistry. The comparison of the two complexes depending on the arene ancillary ligands is our main interest because they possess differences in their symmetry and electron-donating ability as well as structural bulkiness (Chart 2).

Results and Discussion

Synthesis of Coordinatively Unsaturated Metal Complexes. Mononuclear 16-electron arene-ruthenium(II)-dithiolate complexes of the general formula [(η^6-arene)Ru(Cab$^{S,S'}$)] [η^6-arene = *p*-cymene (**3a**),[5] C$_6$Me$_6$ (**3b**)] have been prepared by treatment of the arene ruthenium chloride dimer (**2**) with 2 molar equiv of the corresponding dilithium dithiolato ligand Li$_2$Cab$^{S,S'}$ (**1**), as shown in Scheme 1.

All these monomeric complexes show an intense blue color of the LMCT band due to the donation from the filled S(pπ) orbital to the empty Ru(dπ*) orbital, which

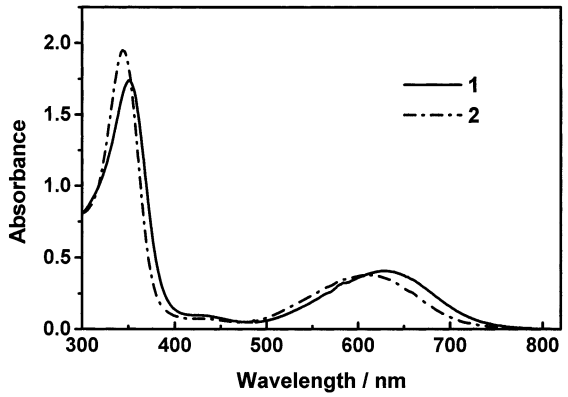

Figure 1. Absorption spectra of 0.25 mM of (η^6-*p*-cymene)-Ru(Cab$^{S,S'}$) (**3a**) and (η^6-C$_6$Me$_6$)Ru(Cab$^{S,S'}$) (**3b**) in CH$_2$Cl$_2$ (light path length 1.0 cm). (1) 0.25 mM **3a** in 0.025 M TBAB CH$_2$Cl$_2$ solution, 350 nm, $\epsilon = 7.0 \times 10^3$ M^{-1} cm^{-1}; 628 nm, $\epsilon = 1.6 \times 10^3$ M^{-1}cm^{-1}. (2) 0.25 mM **3b** in 0.025 M TBAB CH$_2$Cl$_2$ solution, 346 nm, $\epsilon = 7.6 \times 10^3$ M^{-1} cm^{-1}; 608 nm, $\epsilon = 1.5 \times 10^3$ M^{-1}cm^{-1}.

coordinatively stabilizes the unsaturated metal centers,[6] as shown in Figure 1. By changing the ligand from *p*-cymene to hexamethylbenzene, the absorption band of the Ru complex shows a blue shift by 20 nm to near 600 nm. The latter ligand is also expected to be more electron-donating than the former ligand on the basis of the results of our previous study.[3] Such an intense blue color corresponds to the LMCT band of the coordinatively unsaturated ruthenium(II) complexes [(η^6-arene)Ru(SAr)$_2$] (arene = C$_6$H$_6$, *p*-cymene, C$_6$Me$_6$),[7] [(Cp*)Ru(μ-SR)]$_2$,[8] and [Ru(SC$_6$F$_5$)$_2$(PPh$_3$)$_2$],[9] as well as the related [(η^6-*p*-cymene)Os(Cab$^{S,S'}$)][5] and [(Cp*)Ir-(Cab$^{S,S'}$)].[1d] These 16-electron metal complexes **3** are stable in solution; no dimerization is observed in the NMR spectra. In the ^{1}H NMR spectra, even a week after the crystal was dissolved, only one singlet peak of the methyl protons for the *p*-cymene ligand of **3a** or one peak for the protons for the hexamethylbenzene ligand of **3b** was observed. Thus, the analytical and spectroscopic data support the formulation of **3** as a mononuclear 16-electron *o*-carboranyl dithiolate metal complex, and this formulation has been confirmed by an electrochemical study of **3**, which showed coordinative unsaturation in the steric sense around the ruthenium center in the two-legged piano-stool geometry (Chart 2).

Figure 2 shows cyclic voltammograms (CVs) of **3a** (A) and **3b** (B) in CH$_2$Cl$_2$ containing 0.1 M TBAB at the scan rate (v) of 0.1 V s^{-1}. The CV of **3a** shows two major redox responses, i.e., a reversible 0/−1 reduction wave

(5) Herberhold, M.; Yan, H.; Milius, W. *J. Organomet. Chem.* **2000**, *598*, 142.

(6) (a) Michelman, R. I.; Ball, G. E.; Bergmen, R. G.; Anderson, R. A. *Organometallics* **1994**, *13*, 869. (b) Garcia, J. J.; Torrens, H.; Adames, H.; Bailey, N. A.; Scacklady, A.; Matlis, P. M. *J. Chem. Soc., Dalton Trans.* **1993**, 1529. (c) Michelman, R. I.; Anderson, R. A.; Bergman, R. G. *J. Am. Chem. Soc.* **1991**, *113*, 5100. (d) Garcia, J. J.; Torrens, H.; Adams, H.; Bailey, N. A.; Maitlis, P. M. *J. Chem. Soc., Chem. Commun.* **1991**, 74. (e) Klein, D. P.; Kloster, G. M.; Bergman, R. G. *J. Am. Chem. Soc.* **1990**, *112*, 2022.

(7) Mashima, K.; Kaneyoshi, H.; Kaneko, S.; Mikami, A.; Tani, K.; Nakamura, A. *Organometallics* **1997**, *16*, 1016.

(8) (a) Takahashi, A.; Mizobe, Y.; Matsuzaka, H.; Dev, S.; Hidai, M. *J. Organomet. Chem.* **1993**, *456*, 243. (b) Koelle, U.; Rietmann, C.; Englert, U. *J. Organomet. Chem.* **1992**, *423*, C20.

(9) Catala, R.-M.; Cruz-Garritz, D.; Sosa, P.; Terreros, P.; Torrens, H.; Hills, A.; Hughes, D. L.; Richards, R. L. *J. Organomet. Chem.* **1989**, *359*, 219.

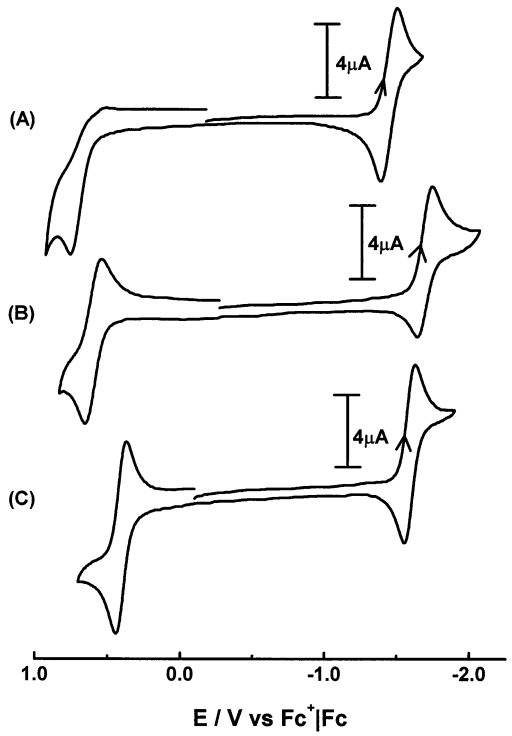

Figure 2. Cyclic voltammograms of 1 mM **3a** (A), **3b** (B, C) at a platinum disk electrode with negative initial scan direction; in CH_2Cl_2 containing 0.1 M TBAB (A, B) and in CH_3CN containing 0.1 M TBAP (C); $v = 0.1$ V s^{-1}.

at $E_{1/2} = -1.45$ V and a virtually chemically irreversible 0/+1 oxidation wave at $E_{pa} = 0.75$ V. The chemical reversibility of redox waves improved with the larger scan rates; thus the 0/−1 and 0/+1 redox couples have been assigned as shown in eq 1.[10] The differences in the peak potentials ($E_{pa} - E_{pc}$) are similar to that of the Fc/Fc^+ couples, i.e., one-electron processes.[11]

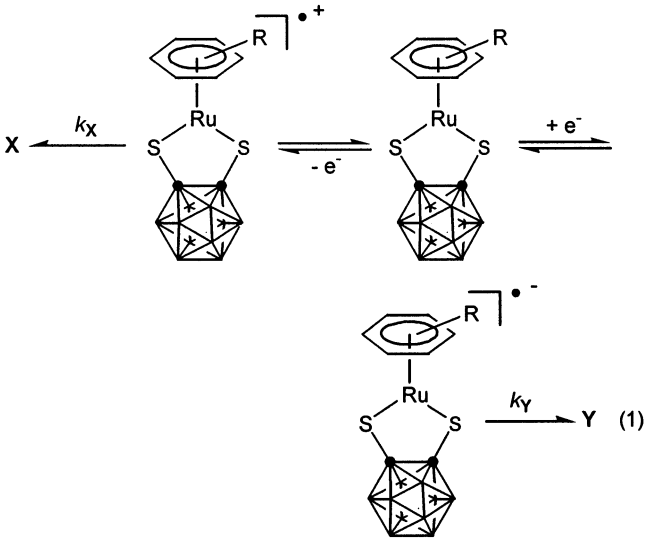

This redox pattern is very similar to those of (η^5-Cp*)M(Cab$^{S,S'}$) (M = Co, Rh, Ir), which was ascribed to the redox properties of the electron-deficient 16-electron complexes.[3] In contrast to the CV of (η^6-*p*-cymene)Ru(Cab$^{S,S'}$), an enhancement in the chemical reversibility of the 0/+1 couples is demonstrated in the CV of (η^6-C_6Me_6)Ru(Cab$^{S,S'}$) in CH_2Cl_2 (Figure 2B) due to the stronger electron-donating ability of hexamethylbenzene than *p*-cymene. In Figure 2B, the ratio of i_{pa}/i_{pc} depending on the scan rate is a diagnostic of the EC mechanism,[12] and the k_Y value (defined in eq 1) is determined as ca. 0.1 s^{-1} by assuming first-order kinetics;[13] that is, the lifetime of the −1 state is ca. 10 s, whereas the k_X value is too small to be determined by the CV technique. However, the CV of **3b** in CH_3CN shows good chemical reversibility in both the oxidation and reduction waves (Figure 2C), where the shifts in redox potentials seemed to be ascribed to the fact that the relative stability of the +1 and −1 states compared with the 0 state increases in a polar solvent.

Synthesis and Characterization of Complexes [(η^6-arene)Ru(Cab$^{S,S'}$)(L)] (arene = *p*-cymene (a), C_6Me_6 (b); L = PEt_3 (4), $CNBu^t$ (5), CO (6)). The reaction of the 16-electron complex **3** with two-electron donor molecules such as triethylphosphine, *tert*-butyl isocyanide, and carbon monoxide proceeded to give various 18-electron complexes, as shown in Scheme 2. Our results are closely related to those of the reported 16-electron cobalt, ruthenium, rhodium, osmium, and iridium complexes such as (η^5-Cp)Co(Cab$^{S,S'}$),[3] (η^6-*p*-cymene)Ru(Cab$^{S,S'}$),[5] (η^5-Cp*)Rh(Cab$^{S,S'}$),[3] (η^6-*p*-cymene)Os(Cab$^{S,S'}$),[5] and (η^5-Cp*)Ir(Cab$^{S,S'}$).[1d]

The reaction of **3** with an excess of PEt_3 in toluene afforded red crystals of **4** in 85−93% yield. The $^{31}P\{^1H\}$ NMR of **4** exhibited a singlet signal at around δ 22−28. The ^1H NMR data for **4** conform to the structure determined by the X-ray structural study. The ORTEP diagram in Figure 3 shows the molecular structure of **4b** and confirms the six-coordinate geometry about the ruthenium atom, assuming that the hexamethylbenzene ring serves as a three-coordinate ligand. The Ru atom environment is transformed from a two-legged piano-stool geometry in **3b** to a three-legged version in **4b**. Overall, the structure is octahedral with an idealized C_s molecular symmetry, similar to what is observed in other related complexes such as [(η^5-Cp)Co(Cab$^{S,S'}$)(PEt_3)],[3] [(η^5-Cp*)Ir(Cab$^{S,S'}$)(PMe_3)],[1d] and (η^6-*p*-cymene)Ru(Cab$^{S,S'}$)(L) (L = PPh_3, $P(OMe)_3$, NH_3, NC_5H_5, CO, $CNBu^t$, SEt_2, SC_4H_8, CN^-, SCN^-).[5]

Treatment of the mononuclear **3** with an excess of $CNBu^t$ in toluene gave a reddish brown addition product [(η^6-arene)Ru(Cab$^{S,S'}$)($CNBu^t$)] (**5**) in 87−91% yield. Complex **5** exhibited a single CN stretching absorption at around 2200 cm^{-1} in the IR spectrum, and this wavenumber is quite normal for a terminal Ru−CNR ligand and significant π-back-bonding of the isocyanide ligand. The ^1H NMR spectrum of **5** indicated a singlet signal at δ 1.5 due to a *tert*-butyl moiety. The structural analysis of **5b** (Figure 4) reveals a molecular core with similarities to that of complex **4b**; the metal center is in a distorted octahedral environment consisting of the carbon atom of the isocyanide ligand with the Ru−C interaction completing the coordination sphere.

(10) Yang, K.; Bott, S. G.; Richimond, M. G. *J. Organomet. Chem.* **1994**, *483*, 7.

(11) A plot of E vs $\log[(i_l - i)/i]$ from the CV of the Fc+/Fc couple using a microdisk (10 μm diameter) showed a slope of 60 mV. But the peak potential difference increased in the present data probably due to the solution resistance.

(12) Nicholson, R. S.; Shain, I. *Anal. Chem.* **1964**, *36*, 706.

(13) Kim, J. Y.; Lee, C.; Park, J. W. *J. Electroanal. Chem.* **2001**, *504*, 104.

Scheme 2. Addition Reaction of 16-Electron Metal Complexes 3[a]

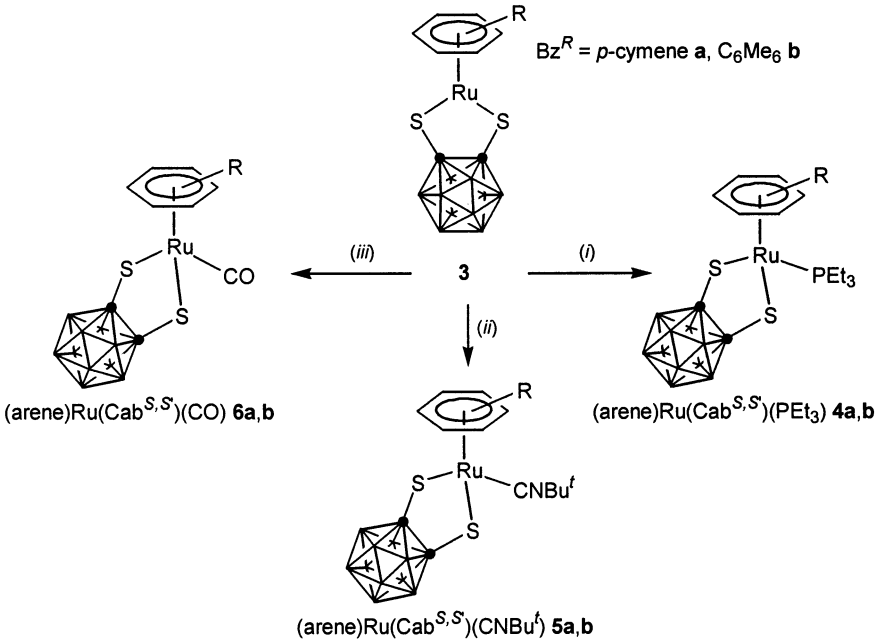

[a] (i) PEt_3, toluene, 25 °C; (ii) $CNBu^t$, toluene, 25 °C; (iii) CO, toluene, 25 °C.

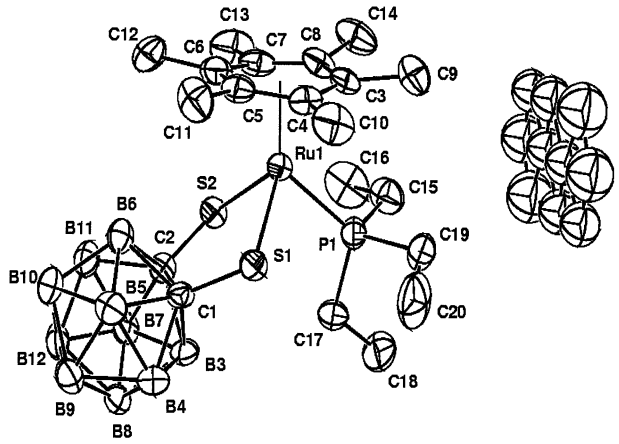

Figure 3. Molecular structure of **4b** with atom labeling; ellipsoids show 30% probability levels and hydrogen atoms have been omitted for clarity.

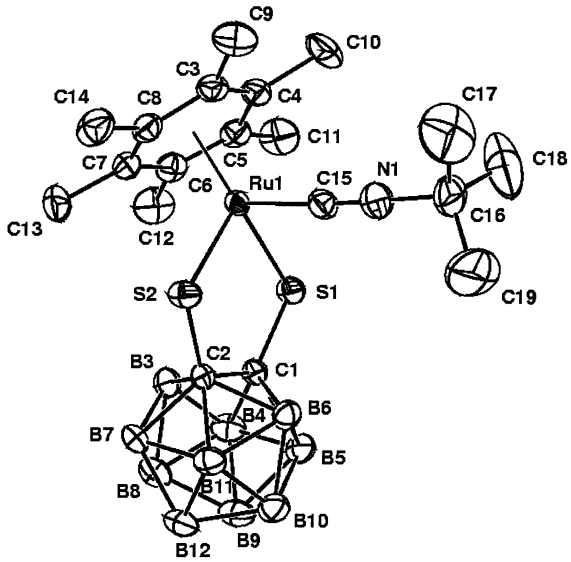

Figure 4. Molecular structure of **5b** with atom labeling; ellipsoids show 30% probability levels and hydrogen atoms have been omitted for clarity.

The treatment of **3b** at atmospheric pressure with carbon monoxide in toluene resulted in the formation of the mononuclear carbonyl adduct [(η^6-C_6Me_6)Ru(Cab$^{S,S'}$)(CO)] (**6b**) in 95% yield. The structure of **6b** was determined on the basis of the spectral data as well as an elemental analysis. The ^{1}H NMR spectrum of **6b** exhibited a single proton signal assignable to a coordinated hexamethylbenzene ligand. The IR spectrum indicates that one carbon monoxide is bound to the ruthenium atom in accordance with the strong ν(CO) band at 1989 cm^{-1}.

The cyclic voltammetric data in CH_2Cl_2 containing 0.1 M TBAB with the scan rate of 0.1 V s^{-1} are summarized in Table 4. The CVs of **4** and **5** show a fully reversible 0/+1 oxidation wave as expected for the 18-electron complexes, and the $E_{1/2}$ values for both 0/+1 and 0/−1 redox waves shift in the negative direction compared with **3**. Almost the same amount of potential shift is observed whether the η^6-arene moiety is η^6-*p*-cymene or η^6-C_6Me_6. The CV patterns of **6a** and **6b** are similar to **3** and **4** except the direction of the potential shifts of the 0/+1 waves.

Reaction of 3a with Arylamines (7). We are interested in extending these studies to tethered arene-ruthenium(II) complexes, from which it might be possible to generate, by replacing the *p*-cymene, the amine strapped arene-ruthenium(II) analogous to the chelation-stabilized phosphine complexes of (arene)ruthenium(II), such as [$RuCl_2$\{η^1:η^6-$R_2P(CH_2)_3$(aryl)\}] (R = Me, Ph; aryl = Ph, 2,4,6-$C_6H_2Me_3$, C_6Me_6),[14] [$RuCl_2$\{η^1:η^6-$Me_2PCH_2SiMe_2C_6H_5$\}],[14] [$RuCl_2$\{η^1:η^6-$Me_2P(CH_2)_3C_6H_5$\}],[15] [$RuCl_2$\{η^1:η^6-$Cy_2P(CH_2)_3C_6H_5$\}],[16] [$RuCl_2$-

(14) Bennett, M. A.; Edwards, A. J.; Harper, J. R.; Khimyak, T.; Willis, A. C. *J. Organomet. Chem.* **2001**, *629*, 7.
(15) Smith, P. D.; Wright, A. H. *J. Organomet. Chem.* **1998**, *559*, 141.

Table 1. X-ray Crystallographic Data and Processing Parameters for Compounds 4b, 5b, 8b, and 11b

	4b	5b	8b	11b
formula	$C_{27}H_{51}B_{10}PS_2Ru$	$C_{19}H_{37}B_{10}NS_2Ru$	$C_{21}H_{37}B_{10}NOS_2Ru$	$C_{36}H_{76}B_{20}S_4Si_2Ru_2$
fw	679.99	552.79	592.81	1111.73
cryst class	monoclinic	triclinic	triclinic	monoclinic
space group	$P2_1/c$	$P\bar{1}$	$P\bar{1}$	$P2_1/n$
Z	4	2	2	4
cell constants				
a, Å	8.9166(4)	11.484(1)	10.8507(7)	20.8410(2)
b, Å	15.912(2)	11.6254(7)	11.7209(8)	10.5570(7)
c, Å	22.492(1)	11.7828(7)	13.3027(9)	25.670(2)
V, Å^3	3191.0(4)	1364.6(2)	1441.6(2)	5492.2(8)
α, deg		66.884(5)	106.870(6)	
β, deg	90.381(4)	82.193(6)	97.023(6)	103.490(6)
γ, deg		70.602(6)	112.586(6)	
μ, cm^{-1}	6.87	7.37	7.06	7.74
cryst size, mm	0.35 × 0.35 × 0.4	0.3 × 0.3 × 0.4	0.35 × 0.4 × 0.5	0.25 × 0.25 × 0.4
D_{calcd}, g/cm^3	1.415	1.345	1.366	1.344
F(000)	1300	568	608	2288
radiation		Mo Kα (λ = 0.7107 Å)		
θ range, deg	1.57−25.97	1.88−25.98	1.66−25.97	1.14−25.97
h, k, l collected	+11, +19, ±27	+14,±14, ±14	+13, ±14, ±16	+25,+13, ±31
no. of reflns collected/unique	6664/6251	5674/5353	5971/5652	11 046/10 740
no. of data/restraints/params	6251/0/331	5353/0/317	5652/0/347	10 732/0/615
goodness-of-fit on F^2	0.962	0.872	1.599	0.907
final R indices [$I > 2\sigma(I)$][a,b]	R_1 = 0.0592	R_1 = 0.0409	R_1 = 0.0842	R_1 = 0.0438
	wR_2= 0.1402	wR_2 = 0.1069	wR_2 = 0.2207	wR_2 = 0.1161
R indices (all data)[a,b]	R_1 = 0.1487	R_1 = 0.0589	R_1 = 0.1157	R_1 = 0.0999,
	wR_2 = 0.1775	wR_2 = 0.1201	wR_2 = 0.2331	wR_2 = 0.1559
largest diff peak and hole, e/Å^3	1.221 and −0.985	1.345 and −0.741	2.746 and −3.792	0.573 and −0.397

[a] $R_1 = \Sigma||F_o| - |F_c||$ (based on reflections with $F_o^2 > 2\sigma F^2$). [b] $wR_2 = [\Sigma[w(F_o^2 - F_c^2)^2]/\Sigma[w(F_o^2)^2]]^{1/2}$; $w = 1/[\sigma^2(F_o^2) + (0.095P)^2]$; $P = [\max(F_o^2, 0) + 2F_c^2]/3$ (also with $F_o^2 > 2\sigma F^2$).

Table 2. Selected Interatomic Distances (Å) in 4b, 5b, 8b, and 11b

		Compound **4b**			
Ru(1)−S(1)	2.3854(18)	Ru(1)−S(2)	2.3975(18)	Ru(1)−C(3)	2.291(7)
Ru(1)−C(4)	2.221(7)	Ru(1)−C(5)	2.358(7)	Ru(1)−C(6)	2.352(8)
Ru(1)−C(7)	2.246(7)	Ru(1)−P(1)	2.320(2)	S(1)−C(1)	1.784(7)
S(2)−C(2)	1.796(7)				
		Compound **5b**			
Ru(1)−S(1)	2.3762(10)	Ru(1)−S(2)	2.3639(9)	Ru(1)−C(3)	2.234(4)
Ru(1)−C(4)	2.226(4)	Ru(1)−C(5)	2.232(4)	Ru(1)−C(6)	2.316(4)
Ru(1)−C(7)	2.318(4)	Ru(1)−C(8)	2.234(4)	Ru(1)−C(15)	1.926(4)
S(1)−C(1)	1.787(3)	S(2)−C(2)	1.785(3)	N(1)−C(15)	1.146(5)
N(1)−C(16)	1.450(6)				
		Compound **8b**			
Ru(1)−S(1)	2.381(2)	Ru(1)−S(2)	2.385(2)	Ru(1)−C(3)	2.243(7)
Ru(1)−C(4)	2.208(8)	Ru(1)−C(5)	2.219(8)	Ru(1)−C(6)	2.227(8)
Ru(1)−C(7)	2.182(9)	Ru(1)−C(8)	2.183(8)	S(1)−C(1)	1.784(8)
S(2)−C(2)	1.801(8)	N(1)−C(13)	1.494(10)		
		Compound **11b**			
Ru(1)−S(1)	2.3185(14)	Ru(1)−S(2)	2.4049(15)	Ru(1)−C(3)	2.267(6)
Ru(1)−C(4)	2.260(6)	Ru(1)−C(5)	2.191(6)	Ru(1)−C(6)	2.239(6)
Ru(1)−C(7)	2.223(6)	Ru(1)−C(8)	2.197(6)	Ru(1)−C(15)	2.142(5)
S(1)−C(1)	1.820(5)	S(2)−C(2)	1.776(6)	S(1)−C(15)	1.781(5)
Si(1)−C(15)	1.877(6)				

{η^1:η^6-1,4-$Cy_2P(CH_2)_2C_6H_4(CH_2OH)$}],[17] and [$RuCl_2$-{$\eta^1$:$\eta^6$-$R_2P(CH_2)_2C_6H_5$}] (R = Ph, Cy).[18] However, we were unable to reproduce Smith and Wright's preparation of [$RuCl_2${η^1:η^6-$Me_2P(CH_2)_3C_6H_5$}][15] from the *p*-cymene complex **3a** in chlorobenzene at 130 °C.

The ^{1}H NMR spectrum showed a broad singlet at δ 5.6. This can be attributed to an intermediate [(η^6-*p*-cymene)Ru(Cab$^{S,S'}$)(arylamine)] (**8**), which, however, decomposed upon prolonged reflux. Contrary to Smith and Wright, we find that the ruthenium dithiolate of an arene, in our case, the *p*-cymene complex **3a**, is not a suitably labile precursor to tethered arene complexes. It reacts with the arylamine ligands (**7**) in a 1:1 mole ratio in dichloromethane at room temperature to quantitatively give the corresponding *N*-bonded adducts **8**, which do not lose the *p*-cymene upon heating in dichloromethane or dichloromethane/THF at 120 °C for 72 h. Therefore, simple base-adducts can be isolated after recrystallization of the crude reaction mixtures in yields

(16) (a) Fürstner, A.; Liebl, M.; Lehmann, C. W.; Picquet, M.; Kunz, R.; Bruneau, C.; Touchard, D.; Dixneuf, P. H. *Chem. Eur. J.* **2000**, *6*, 1847. (b) Jan, D.; Delaude, L.; Simal, F.; Demonceau, A.; Noels, A. F. *J. Organomet. Chem.* **2000**, *606*, 55. (c) Simal, F.; Jan, D.; Demonceau, A.; Noels, A. F. *Tetrahedron Lett.* **1999**, *40*, 1653.

(17) (a) Therrien, B.; Ward, R. *Angew. Chem., Int. Ed.* **1999**, *38*, 405. (b) Therrien, B.; König, A.; Ward, T. R. *Organometallics* **1999**, *18*, 1565. (c) Therrien, B.; Ward, T. R.; Pilkington, M.; Hoffmann, C.; Gilardoni, F.; Weber, J. *Organometallics* **1998**, *17*, 330.

(18) Abele, A.; Wurshe, R.; Klinga, M.; Rieger, B. *J. Mol. Catal. A* **2000**, *160*, 23.

Table 3. Selected Interatomic Angles (deg) in 4b, 5b, 8b, and 11b

		Compound **4b**			
P(1)−Ru(1)−S(1)	87.38(7)	P(1)−Ru(1)−S(2)	89.52(7)	S(1)−Ru(1)−S(2)	86.78(6)
C(1)−S(1)−Ru(1)	106.5(2)	C(2)−S(2)−Ru(1)	106.2(2)	C(15)−P(1)−Ru(1)	114.7(3)
C(17)−P(1)−Ru(1)	117.7(3)	C(19)−P(1)−Ru(1)	116.5(3)		
		Compound **5b**			
C(15)−Ru(1)−S(2)	88.75(12)	C(15)−Ru(1)−S(1)	87.07(12)	S(2)−Ru(1)−S(1)	89.99(3)
C(1)−S(1)−Ru(1)	105.77(12)	C(2)−S(2)−Ru(1)	106.06(12)	C(15)−N(1)−C(16)	176.9(5)
N(1)−C(15)−Ru(1)	176.1(4)				
		Compound **8b**			
N(1)−Ru(1)−S(1)	85.1(2)	N(1)−Ru(1)−S(2)	82.46(1)	S(1)−Ru(1)−S(2)	88.83(7)
C(1)−S(1)−Ru(1)	106.7(2)	C(2)−S(2)−Ru(1)	106.6(2)	C(13)−N(1)−Ru(1)	122.2(5)
N(1)−C(13)−C(14)	114.1(6)	C(15)−C(14)−C(13)	112.5(7)	C(20)−C(15)−C(16)	119.0(8)
C(20)−C(15)−C(14)	121.6(7)				
		Compound **11b**			
C(15)−Ru(1)−S(1)	46.85(14)	C(15)−Ru(1)−S(2)	85.94(15)	S(1)−Ru(1)−S(2)	87.59(5)
C(15)−S(1)−C(1)	108.8(3)	C(15)−S(1)−Ru(1)	61.4(2)	C(1)−S(1)−Ru(1)	108.9(2)
C(2)−S(2)−Ru(1)	106.0(2)	S(1)−C(15)−Si(1)	113.2(3)	S(1)−C(15)−Ru(1)	71.8(2)
Si(1)−C(15)−Ru(1)	139.9(3)				

Table 4. Cyclic Voltammetric Data for 3 and Their Derivatives[a]

	redox couple[b] 0/+1				redox couple[b] 0/−1			
	E_{pa}	E_{pc}	i_{pc}/i_{pa}	$E_{1/2}$	E_{pa}	E_{pc}	i_{pa}/i_{pc}	$E_{1/2}$
3a	0.75	0.65		0.70	−1.39	−1.51	1	−1.45
3b	0.65	0.54	1	0.60	−1.65	−1.75	0.70	−1.70
4a	0.37	0.28	1	0.33	c	−2.41		−2.35[d]
4b	0.31	0.21	1	0.26	*e*	*e*	*e*	*e*
5a	0.57	0.48	1	0.53	*c*	−2.21		−2.16[d]
5b	0.44	0.35	1	0.40	*c*	−2.41		−2.36[d]
6a	0.97	c	0.21	0.93[d]	*c*	−1.70		−1.65[d]
6b	0.89	0.76	1	0.83	*c*	−2.26		−2.21[d]
9a	0.58	0.50	0.51	0.54	−1.76	−1.91		−1.84
9b	0.47	0.36	1	0.42	*c*	−2.17		−2.12[d]
10b	0.16	0.07	1	0.12	*c*	−2.46		−2.41[d]

[a] All cyclic valtammograms were recorded at rt at a scan rate of 0.1 V s^{-1}, and potentials are in volts vs $Fc^+|Fc$ couple. [b] E_{pa} and E_{pc} refer to the anodic and cathodic peak potentials for a given redox couple. [c] No reverse redox peaks was observed. [d] $E_{1/2}$ is calibrated with $E_{1/2} = E_{pa} - (\Delta E_p, Fc^+|Fc)/2$ [e] Reduction wave outside the solvent window

ranging from 86 to 91% for [(η^6-*p*-cymene)Ru(Cab$^{S,S'}$)-(L)] (**8**) [L = η^1-$NH_2(CH_2CH_2)$Ar, Ar = C_6H_5 (**8a**); C_6H_4OMe (**8b**); $C_6H_3(OMe)_2$ (**8c**); C_8H_6N (**8d**)], as shown in Scheme 3.

The NMR spectra of the arylamine complexes show, in addition to resonances characteristic of the coordinated NH_2 group, resonances due to the protons of the free arene ring in the region of δ 6.7−7.6 and corresponding resonances due to the aromatic carbon atoms in the region of δ 110−160. The *N*-methyl groups in **8** are nonequivalent because of the diasterotopicity of the arylamines and appear as two doublets in the $^{13}C\{^1H\}$ and ^1H NMR spectra. The molecular structure of the arylamine-coordinated ruthenium dithiolates **8b** has been determined by a single-crystal X-ray analysis and is shown with atom labeling in Figure 5. It confirms the six-coordinate geometry about the ruthenium center, assuming that the arylamine ligand functions as a monodentate ligand. The *N*-methylene chain is not in a fully extended conformation but is nonetheless oriented such that the aminoalkyl unit is held remote from the ruthenium fragment. The CVs of **8a**,**b**,**d** showed an apparently reversible reduction and a more prominent but chemically irreversible oxidation; however, the instability of **8** limited electrochemical studies (see Supporting Information).

Insertion of Ru−S Bonds of 3. It is recognized that π donation by a lone pair of electrons on the coordinated sulfur atom alleviates such an electron deficiency and thus the coordinative unsaturation around the transition metal center. Consequently, this geometry suggests that some multiple-bond character is present in the Ru−S bonds of complex **3**. To verify the nature of the Ru−S bonds, the insertion reactions of several organic and organometallic compounds to **3** have been investigated. Indeed, complex **3** was found to be a good precursor for other insertion reactions.[19,20] The treatment of **3** with 1−2 equiv of an alkyne in refluxing benzene for 2 h gave the alkyne insertion complexes [(η^6-arene)Ru{η^3-(*S*,*S*,*C*′)-$SC_2B_{10}H_{10}SC'R_2$}] [C′R_2 = (COOMe)C═C(COOMe) (**9**: arene = *p*-cymene (**9a**), C_6Me_6 (**9b**)), HC═CPh (**10**: arene = C_6Me_6 (**10b**))], in moderate yield (Scheme 4).

The IR spectra of **9** exhibit one ν(C═C) stretching band, and the ^1H NMR spectra of **9** display the characteristic resonances of a coordinated olefin. Thus, for **9**, the O*Me* groups of the ester give rise to two singlets centered at δ 3.72 and 3.83, respectively. For the $^{13}C\{^1H\}$ NMR spectra of **9**, it is sufficient to point out that the resonances due to the π-bound olefin carbons are characteristically upfield-shifted. The spectroscopic data of the ruthenium complexes are in complete agreement with the proposed structure of **9**. Although the process outlined in Scheme 4 proved quite general, there were, however, structural limitations observed for the metallabicyclic complexes **10**.[1b,21] For example, several attempts to synthesize the complexes **10a** with phenyl acetylene were unsuccessful, yielding only decomposition under prolonged reflux conditions. The conversion of **3** to the corresponding metallabicyclic complexes

(19) (a) Takayama, C.; Takeuchi, K.; Kajitani, M.; Sugiyama, T.; Sugimori, A. *Chem. Lett.* **1998**, 241. (b) Sakurada, M.; Kajitani, M.; Dohki, K.; Akiyama, T.; Sugimori, A. *J. Organomet. Chem.* **1992**, *423*, 141. (c) Sakurada, M.; Okubo, J.; Kajitani, M.; Akiyama, T. Sugimori, A. *Phosphorus, Sulfur, Silicon, Relat. Elements* **1992**, *67*, 145. (d) Kajitani, M.; Sakurada, M.; Dohki, K.; Suetsugu, T.; Akiyama, T.; Sugimori, A. *J. Chem. Soc., Chem. Commun.* **1990**, 19. (e) Sakurada, M.; Okubo, J.; Kajitani, M.; Akiyama, T.; Sugimori, A. *Chem. Lett.* **1990**, 1837.

(20) (a) Kajitani, M.; Suetsugu, T.; Takagi, T.; Akiyama, T.; Sugimori, A.; Aoki, K.; Yamazaki, H. *J. Organomet. Chem.* **1995**, *487*, C8. (b) Sakurada, M.; Kajitani, M.; Dohki, K.; Akiyama, T.; Sugimori, A. *J. Organomet. Chem.* **1992**, *423*, 141. (c) Kajitani, M.; Suetsugu, T.; Wakabayashi, R.; Igarashi, A.; Akiyama, T.; Sugimori, A. *J. Organomet. Chem.* **1985**, *293*, C15.

Scheme 3. Addtion Reaction of 16-Electron Metal Complex 3a[a]

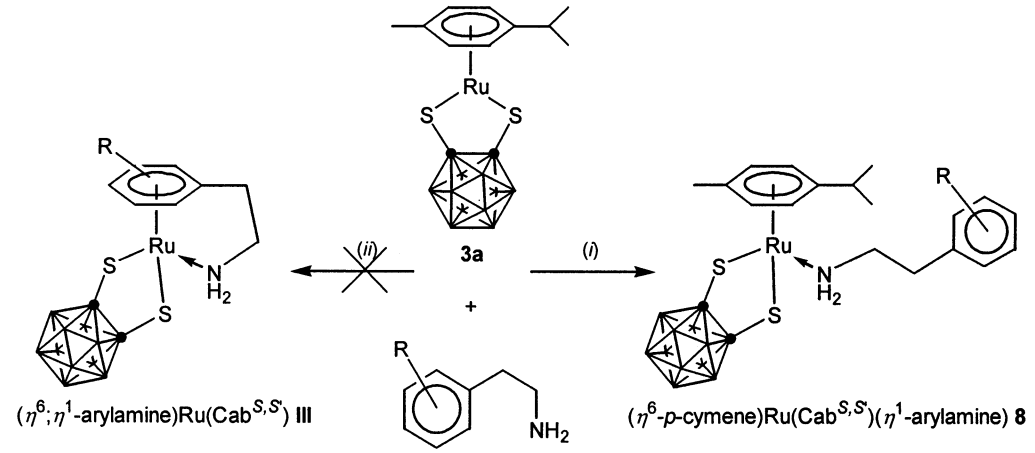

[a] (i) CH_2Cl_2, 25 °C; (ii) Ch_2Cl_2/THF, 120 °C.

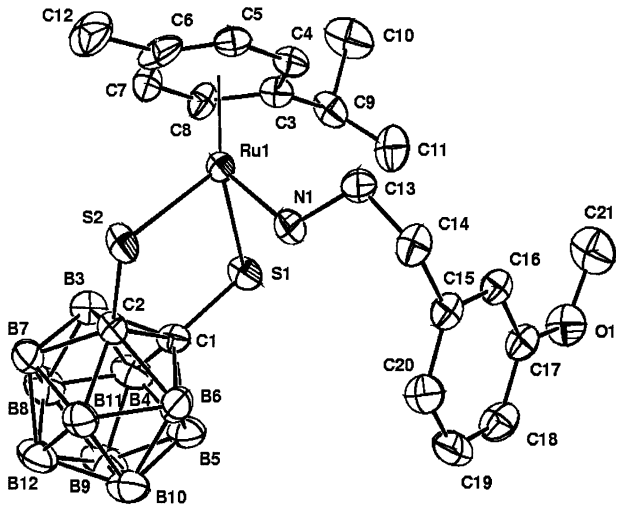

Figure 5. Molecular structure of **8b** with atom labeling; ellipsoids show 30% probability levels and hydrogen atoms have been omitted for clarity.

9 or **10** is generally favored by the electron-rich ruthenium complex; therefore, we decided to investigate the reactivity of **3b** toward the less reactive phenyl acetylene. Indeed, complex **10b** was produced in high yields from the direct two-carbon insertion reaction of phenyl acetylene with complex **3b**. The ^{1}H NMR spectrum of **10b** shows the terminal proton at δ 6.42 and multiplet signals (δ 7.30) of the phenyl group of the acetylene.

At v of 0.1 V s^{-1}, the CV of **9a** does not show an entire chemical reversibility of 0/+1 oxidation, while that of **9b** does show a fully reversible 0/+1 oxidation wave (Table 4). The same trend is shown in the CVs of **10b**. However, the amounts of the redox potential shifts imply that −CH=CPh− acts as a stronger ligand than −COOMeC=CCOOMe−.

Similar to the reactions between **3** and alkynes, the ruthenadithia-*o*-carborane ring in **3** undergoes the insertion of a methylene group between Ru and S in its reaction with a diazoalkane. The reaction of **3** with $SiMe_3CHN_2$ rapidly occurred at 0 °C, accompanied by the vigorous evolution of N_2 to yield the methylene unit inserted product [(η^6-arene)Ru{η^3-(*S*,*S*,*C*′)-$SC_2B_{10}H_{10}$-SCH_2SiMe_3}] (**11**: arene = *p*-cymene **11a**, C_6Me_6 **11b**), as shown in Scheme 4. The ^{1}H NMR spectrum of complex **11** exhibits resonances for a trimethylsilyl group at δ 0.2 and methine proton δ 3.5. The ^{13}C NMR spectrum also corresponds to the Ru−S-inserted structure: two types of alkyl carbons of the *p*-cymene ring and carbon atoms of the Ru−S-substituted trimethylsilyl methine unit.

To establish the exact conformation of the adduct, the structure of **11b** was determined by a single-crystal X-ray analysis (Figure 6). The X-ray structure of **11b** shows that the ruthenium takes a three-legged pianostool configuration with a bicyclometallacyclic ring. This is due to the insertion of the coordinated dithiolato ligand at the ruthenium(II) metal center. In **11b**, the trimethylsilyl group is located in the anti-position with respect to the ruthenadithia-*o*-carborane ring. The formation of a methylene bridge between a metal and a chalcogen in the reaction with a diazoalkane compound is a typical result due to unsaturation.[20] These cycloaddition reactions suggest that a certain degree of multiple-bond character is present in the Ru−S bond of complex **3b**.

Conclusion

Our electrochemical study of complex **3** with our previous work[3] provided the data pool of the electrochemical behavior accompanying *o*-carboranyl complexes, 16-electron metalladithiolates, depending on the arene or Cp/Cp* ancillary ligands. The π donation from the filled pπ orbital of the sulfur atom to the empty dπ orbital of the metal atom is found to significantly stabilize this unsaturation. Thus, complex **3** is susceptible to the insertion of organic and organometallic compounds into the Ru−S bond of **3**. In addition, this compound exhibits a remarkable reactivity toward

(21) (a) Herberhold, M.; Yan, H.; Milius, W.; Wrackmeyer, B. *J. Chem. Soc., Dalton Trans.* **2001**, 1782. (b) Herberhold, M.; Yan, H.; Milius, W.; Wrackmeyer, B. *J. Organomet. Chem.* **2001**, *623*, 149. (c) Herberhold, M.; Yan, H.; Milius, W.; Wrackmeyer, B. *Organometallics* **2000**, *19*, 4289. (d) Herberhold, M.; Yan, H.; Milius, W.; Wrackmeyer, B. *J. Organomet. Chem.* **2000**, *604*, 170. (e) Herberhold, M.; Yan, H.; Milius, W.; Wrackmeyer, B. *Chem. Eur. J.* **2000**, *6*, 3026. (f) Herberhold, M.; Yan, H.; Milius, W.; Wrackmeyer, B. *Z. Anorg. Allg. Chem.* **2000**, *626*, 1627. (g) Herberhold, M.; Yan, H.; Milius, W.; Wrackmeyer, B. *Angew. Chem., Int. Ed.* **1999**, *38*, 3689. (h) Herberhold, M.; Jin, G.-X.; Yan, H.; Milius, W.; Wrackmeyer, B. *Eur. J. Inorg. Chem.* **1999**, 873. (i) Herberhold, M.; Jin, G.-X.; Yan, H.; Milius, W.; Wrackmeyer, B. *J. Organomet. Chem.* **1999**, *587*, 252.

Scheme 4. Insertion Reaction of 16-Electron Metal Complexes 3[a]

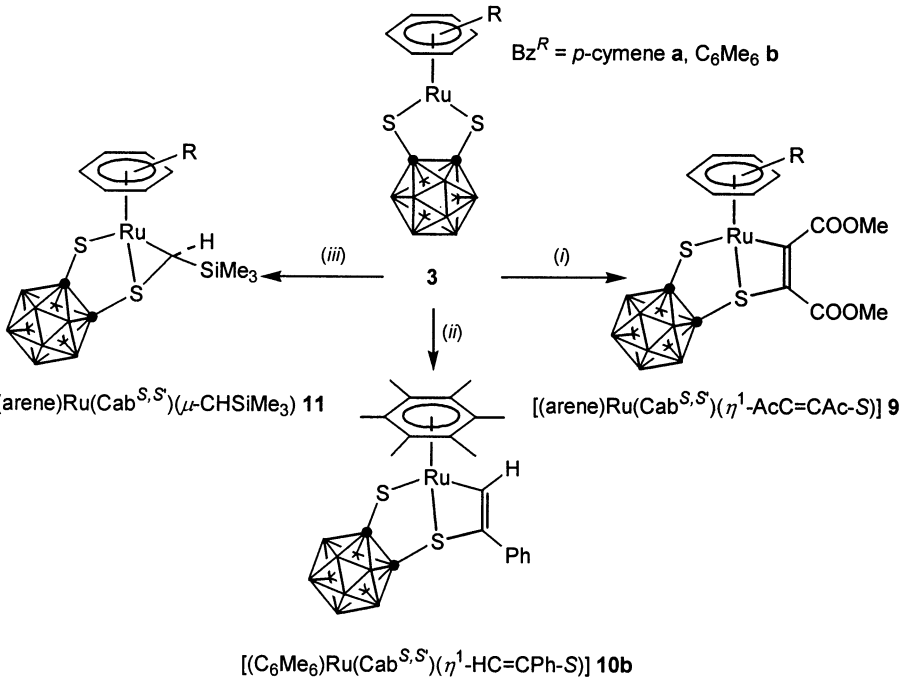

[a] (i) (COOMe)CC(COOMe), toluene, 110 °C; (ii) HCCPh, toluene, 110 °C; (iii) Me_3SiCHN_2, toluene, 25 °C.

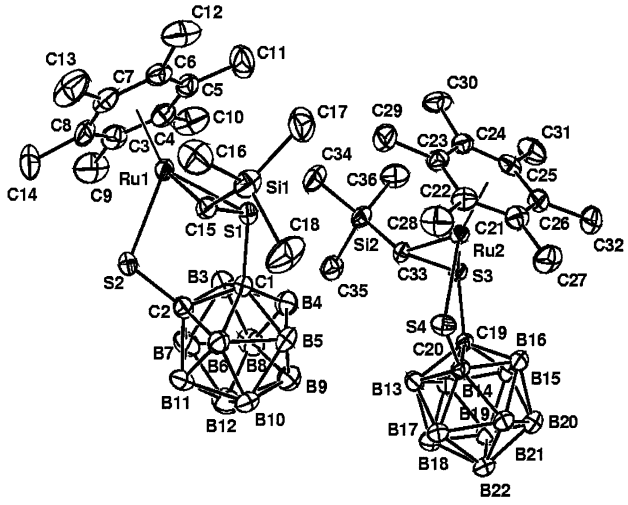

Figure 6. Molecular structure of **11b** with atom labeling; ellipsoids show 30% probability levels and hydrogen atoms have been omitted for clarity.

various nucleophiles such as PEt_3, $CNBu^t$, and CO. In the present study, we tried to relate the electrochemical behavior of the products with the structures analyzed by other spectroscopic data, which can provide much information about their structure at least in metalladithiolate complexes.

Experimental Section

General Procedures. All manipulations were performed under a dry, oxygen-free, nitrogen or argon atmosphere using standard Schlenk techniques or in a Vacuum Atmosphere HE-493 drybox. THF was freshly distilled over potassium benzophenone. Toluene was dried and distilled from sodium benzophenone. Dichloromethane and hexane were dried and distilled over CaH_2. ^1H, ^{13}C, and ^{31}P NMR spectra were recorded on a Varian Mercury 300 spectrometer operating at 300.1, 75.4, and 121.4 MHz, respectively. All proton and carbon chemical shifts were measured relative to internal residual benzene from the lock solvent (99.5% C_6D_6) and then referenced to Me_4Si (0.00 ppm). The ^{31}P NMR spectra were recorded with 85% H_3PO_4 as an external standard. IR spectra were recorded on a Biorad FTS-165 spectrophotometer. Elemental analyses were performed with a Carlo Erba Instruments CHNS-O EA1108 analyzer. All melting points were uncorrected. All the electrochemical measurements were carried out in CH_2Cl_2 or CH_3CN solutions containing 1 mM metal complex and 0.1 M tetrabutylammonium fluoroborate (TBAB), unless otherwise specified, at room temperature using a BAS 100B electrochemical analyzer. For use of CH_3CN solution, tetrabutylammonium perchlorate (TBAP) was used as supporting electrolyte. A platinum disk (diameter 1.6 mm) and platinum wire were used as a working and counter electrode. The reference electrode used was $Ag|AgNO_3$, and all the potential values shown were calibrated vs $Fc^+|Fc$ redox couple, unless otherwise specified. E_{pa} and E_{pc} denote anodic and cathodic peak potential, respectively, and $E_{1/2}$ value indicated is the average of E_{pa} and E_{pc} for the reversible redox waves.

o-Carborane was purchased from the Katechem (Czech Republic) and used without purification. Complex $Cab^{S,S'}$ (**1**),[22] $[(\eta^6\text{-}p\text{-cymene})Ru(\mu\text{-Cl})(Cl)]_2$,[23] and $[(\eta^6\text{-}C_6Me_6)Ru(\mu\text{-Cl})(Cl)]_2$[24] were prepared according to the literature methods.

Preparation of $[(\eta^6\text{-arene})Ru(Cab^{S,S'})]$ [3: arene = *p*-cymene (3a), C_6Me_6 (3b); $Cab^{S,S'} = 1,2\text{-}S_2C_2B_{10}H_{10}\text{-}S,S'$]. Representative procedure: A 3.2 mmol solution of **1** in THF (20 mL) was added to a stirred solution of $[(\eta^6\text{-}p\text{-cymene})Ru(\mu\text{-Cl})(Cl)]_2$ (**2a**) (0.92 g, 1.5 mmol) in THF (30 mL) cooled to −78 °C. The reaction mixture was then allowed to react at 0 °C for 1 h, and the solution was stirred for another 2 h at room temperature. The solution gradually turned dark blue, suggesting the formation of an *o*-carboranyl dithiolato metal complex. The solution was reduced in vacuo to about half its original volume, and some insoluble material was removed by filtration. The solution was removed under vacuum, and the

(22) Smith, H. D., Jr.; Obenland, C. O.; Papetti, S. *Inorg. Chem.* **1966**, *5*, 1013.
(23) Bennett, M. A.; Huang, T.-N.; Matheson, T. W.; Smith, A. K. *Inorg. Synth.* **1982**, *21*, 74.
(24) Crochet, P.; Demerseman, B.; Rocaboy, C.; Schleyer, D. *Organometallics* **1996**, *15*, 3048.

resulting residue was taken up in a minimum of methylene chloride and then transferred to a column of silica gel. The crude residue was purified by column chromatography, affording >98% pure complex as blue crystals. Dark blue crystals of **3a** were formed in 53% yield (0.70 g, 1.6 mmol). Data for **3a**. Anal. Calcd for $C_{12}H_{24}B_{10}S_2Ru$: C, 32.64; H, 5.48. Found: C, 32.72; H, 5.55. IR (KBr, cm^{-1}): ν(B−H) 2589. ^1H NMR (300.1 MHz, ppm, $CDCl_3$): 5.57 (s, 4H, C_6H_4), 2.90 (sp, 1H, C*H*Me$_2$), 2.20 (s, 3H, C*H*$_3$), 1.26 (d, 6H, CH*Me*$_2$, J_{H-H} = 6.9 Hz). $^{13}C\{^1H\}$ NMR (75.4 MHz, ppm, $CDCl_3$): 104.2 (s, C_6H_4), 94.11 (s, C_6H_4), 81.75 (s, C_6H_4), 79.48 (s, C_6H_4), 33.8 (s, *C*HMe$_2$), 31.97 (s, *C*H$_3$), 24.23 (s, CH*Me*$_2$).

3b. **3b** was prepared from 1.00 g (1.5 mmol) of [(η^6-C_6Me_6)-Ru(μ-Cl)(Cl)]$_2$. After flash chromatography on silica gel with hexane/$CHCl_3$ (90:10), **3b** (0.92 g, 2.0 mmol, 65%) was isolated as a blue solid. Data for **3b**. Anal. Calcd for $C_{14}H_{28}B_{10}S_2Ru$: C, 35.8; H, 6.01. Found: C, 35.92; H, 5.95. IR (KBr, cm^{-1}): ν(B−H) 2580. ^1H NMR (300.1 MHz, ppm, $CDCl_3$): 2.21 (s, 18H, C_6Me_6). $^{13}C\{^1H\}$ NMR (75.4 MHz, ppm, $CDCl_3$): 91.88 (s, C_6Me_6), 17.61 (s, C_6Me_6).

General Procedure for the Preparation of 18-Electron Complexes [(η^6-arene)Ru(Cab$^{S,S'}$)(L)] (arene = *p*-cymene, C_6Me_6; L = PEt$_3$, CNBu^t, CO) (4−6). Under argon, ligand L (2.0 mmol) was added to a blue solution of complex **3** (0.23 mmol) in 10 mL of THF. The resultant yellow solution was stirred for 30 min and evaporated to dryness. The yellow residue of the product was dried in vacuo. Spectroscopic data are presented in the Supporting Information.

4a. Yield: 0.12 g (0.21 mmol, 93%). Anal. Calcd for $C_{18}H_{39}B_{10}S_2RuP$: C, 38.62; H, 7.02. Found: C, 38.75; H, 7.10. IR (KBr, cm^{-1}): ν(B−H) 2585, ν(P−C) 1035.

4b: Yield: 85%. Anal. Calcd for $C_{20}H_{43}B_{10}S_2RuP$: C, 40.87; H, 7.37. Found: C, 41.00; H, 7.48. IR (KBr, cm^{-1}): ν(B−H) 2592.

5a. Yield: 91%. Anal. Calcd for $C_{17}H_{33}B_{10}S_2RuN$: C, 38.91; H, 6.34; N, 2.67. Found: C, 39.00; H, 6.40; N, 2.73. IR (KBr, cm^{-1}): ν(B−H) 2580, ν(C═N) 2166. **5b**: Yield: 87%. Anal. Calcd for $C_{19}H_{37}B_{10}S_2RuN$: C, 41.28; H, 6.75; N, 2.53. Found: C, 41.35; H, 6.83; N, 2.60. IR (KBr, cm^{-1}): ν(B−H) 2595, ν(C═N) 2208.

6a. Yield: 91%. Anal. Calcd for $C_{13}H_{24}B_{10}S_2RuO$: C, 33.25; H, 5.15. Found: C, 33.40; H, 5.30. IR (KBr, cm^{-1}): ν(B−H) 2632, 2587, 2560, ν(CO) 2012.

6b: Yield: 95%. Anal. Calcd for $C_{15}H_{28}B_{10}S_2RuO$: C, 36.20; H, 5.67. Found: C, 36.28; H, 5.72. IR (KBr, cm^{-1}): ν(B−H) 2598, ν(CO) 1989.

General Reactions of 3a with Arylamines. In a typical run **3a** (0.44 g, 1.0 mmol) and arylamines (**7**) were dissolved in methylene chloride (15 mL) under argon, and the solution was stirred for 8 h at room temperature. The blue color of the solution slowly faded to give an orange-yellow solution, suggesting the formation of an adduct. The completion of the reaction was monitored by TLC. The solution was reduced in vacuo to about half its original volume, and some insoluble material was removed by filtration. Addition of hexane to the resulting solution afforded **8** as a dark yellow precipitate.

Analytical Data for 8a. 8a was prepared from 2.0 mmol (0.24 mL) of arylamine **7a**. After recrystallization from toluene, **8a** (0.48 g, 0.86 mmol, 86% yield) was isolated as a yellow solid. Carbon atoms and the attached hydrogen atoms are numbered as shown below. Anal. Calcd for $C_{20}H_{35}B_{10}S_2NRu$: C, 42.68; H, 6.26; N, 2.49. Found: C, 42.75; H, 6.30; N, 2.40. IR (KBr, cm^{-1}): ν(B−H) 2590. ^1H NMR (300.1 MHz, ppm, $CDCl_3$): 7.39−7.17 (m, 5H, C4−8), 5.22, 5.08 (AA′BB′, 4H, C_6H_4, J_{Ha-Hb} = 5.1 Hz, $J_{Ha'-Hb'}$ = 6.0 Hz), 2.98 (t, 2H, C1, J_{H-H} = 6.9 Hz), 2.80 (t, 2H, C2, J_{H-H} = 6.9 Hz), 2.62 (sp, 1H, C*H*Me$_2$), 2.18 (s, 3H, C*H*$_3$), 1.12 (d, 6H, CH*Me*$_2$, J_{H-H} = 6.9 Hz). $^{13}C\{^1H\}$ NMR (75.4 MHz, ppm, $CDCl_3$): 137.02 (s, C3), 129.64 (s, C7), 129.40 (s, C5), 128.92 (s, C8), 128.31 (s, C4), 127.84 (s, C6), 107.50 (s, C_6H_4), 100.77 (s, C_6H_4), 93.91 (s, C_6H_4), 31.34 (s, C1), 30.01 (s, C2), 23.30 (s, *C*HMe$_2$), 22.51 (s, *C*H$_3$), 18.87 (s, CH*Me*$_2$).

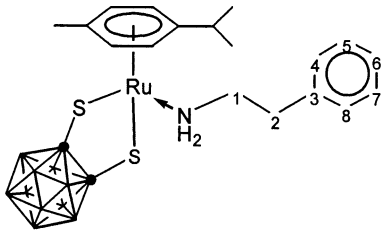

(η^1-arylamine)Ru(Cab$^{S,S'}$) **8a**

Analytical Data for 8b. 8b was prepared from 2.0 mmol (0.29 mL) of arylamine **7b**. After recrystallization from toluene, **8b** (0.52 g, 0.88 mmol, 88% yield) was isolated as a yellow solid. Carbon atoms and the attached hydrogen atoms are numbered as shown below. Anal. Calcd for $C_{21}H_{38}B_{10}S_2NRuO$: C, 42.55;

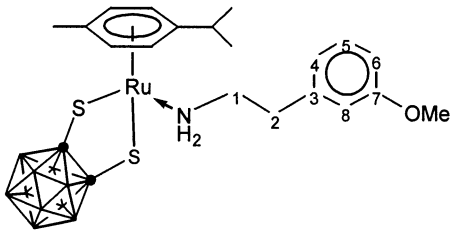

(η^1-arylamine)Ru(Cab$^{S,S'}$) **8b**

H, 6.29; N, 2.36. Found: C, 42.65; H, 6.40; N, 2.40. IR (KBr, cm^{-1}): ν(B−H) 2580. ^1H NMR (300.1 MHz, ppm, $CDCl_3$): 7.31−6.71 (m, 4H, C8, C4−6), 5.22, 5.07 (AA′BB′, 4H, C_6H_4, J_{Ha-Hb} = 6.0 Hz, $J_{Ha'-Hb}$ = 6.0 Hz), 3.83 (s, 3H, O*Me*), 2.97 (t, 2H, C1, J_{H-H} = 6.0 Hz), 2.78 (t, 2H, C2, J_{H-H} = 6.0 Hz), 2.65 (sp, 1H, C*H*Me$_2$), 2.17 (s, 3H, C*H*$_3$), 1.13 (d, 6H, CH*Me*$_2$, J_{H-H} = 6.9 Hz). $^{13}C\{^1H\}$ NMR (75.4 MHz, ppm, $CDCl_3$): 160.27 (s, C7), 138.57 (s, C3), 130.79 (s, C5), 121.92 (s, C4), 113.95 (s, C8), 111.67 (s, C6), 107.50 (s, C_6H_4), 100.86 (s, C_6H_4), 93.95 (s, C_6H_4), 56.32 (s, O*Me*), 31.69 (s, C1), 29.98 (s, C2), 23.23 (s, *C*HMe$_2$), 22.50 (s, *C*H$_3$), 18.84 (s, CH*Me*$_2$).

Analytical Data for 8c. 8c was prepared from 2.0 mmol (0.34 mL) of arylamine **7c**. After recrystallization from toluene, **8c** (0.54 g, 0.87 mmol, 87% yield) was isolated as a yellow solid. Carbon atoms and the attached hydrogen atoms are numbered as shown below. Anal. Calcd for $C_{22}H_{41}B_{10}S_2NRuO_2$: C, 42.42;

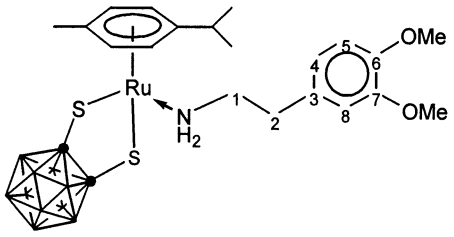

(η^1-arylamine)Ru(Cab$^{S,S'}$) **8c**

H, 6.31; N, 2.25. Found: C, 42.53; H, 6.45; N, 2.19. IR (KBr, cm^{-1}): ν(B−H) 2580. ^1H NMR (300.1 MHz, ppm, $CDCl_3$): 6.87−6.67 (m, 3H, C4, C7−8), 5.23, 5.09 (AA′BB′, 4H, C_6H_4, J_{Ha-Hb} = 6.0 Hz, $J_{Ha'-Hb'}$ = 6.0 Hz), 3.91 (s, 3H, O*Me*), 3.88 (s, 3H, O*Me*), 2.95 (t, 2H, C1, J_{H-H} = 6.0 Hz), 2.75 (t, 2H, C2, J_{H-H} = 6.0 Hz), 2.65 (sp, 1H, C*H*Me$_2$), 2.18 (s, 3H, CH_3), 1.14 (d, 6H, CH*Me*$_2$, J_{H-H} = 7.8 Hz). $^{13}C\{^1H\}$ NMR (75.4 MHz, ppm, $CDCl_3$): 149.60 (s, C7), 148.48 (s, C6), 129.32 (s, C3), 121.89 (s, C4), 112.68 (s, C5), 111.16 (s, C8), 107.44 (s, C_6H_4), 100.77 (s, C_6H_4), 93.84 (s, C_6H_4), 56.76 (s, O*Me*), 55.60 (s, O*Me*), 31.80 (s, C1), 30.09 (s, C2), 23.24 (s, *C*HMe$_2$), 22.53 (s, *C*H$_3$), 18.92 (s, CH*Me*$_2$).

Analytical Data for 8d. 8d was prepared from 2.0 mmol (0.32 g) of arylamine **7d**. After recrystallization from toluene, **8d** (0.55 g, 0.91 mmol, 91% yield) was isolated as a yellow solid.

Carbon atoms and the attached hydrogen atoms are numbered as shown below. Anal. Calcd for $C_{22}H_{36}B_{10}S_2N_2Ru$: C, 43.91;

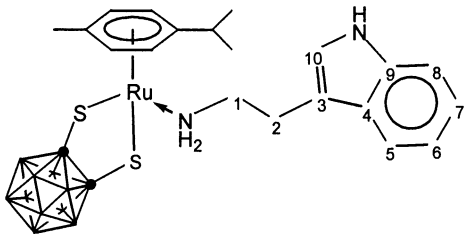

(η^1-arylamine)Ru(Cab$^{S,S'}$) **8d**

H, 6.03; N, 4.65. Found: C, 44.05; H, 6.00; N, 4.60. IR (KBr, cm^{-1}): ν(B−H) 2580. ^{1}H NMR (300.1 MHz, ppm, $CDCl_3$): 7.56−7.14 (m, 5H, C5−8, C10), 5.11, 5.00 (AA′BB′, 4H, C_6H_4, $J_{Ha-Hb} = 6.0$ Hz, $J_{Ha'-Hb'} = 6.0$ Hz), 3.05 (t, 2H, C1, $J_{H-H} = 6.0$ Hz), 2.95 (t, 2H, C2, $J_{H-H} = 6.0$ Hz), 2.36 (sp, 1H, C*H*Me$_2$), 2.12 (s, 3H, CH_3), 0.95 (d, 6H, CH*Me*$_2$, $J_{H-H} = 6.9$ Hz). ^{13}C{^{1}H} NMR (75.4 MHz, ppm, $CDCl_3$): 151.15 (s, C9), 145.52 (s, C4), 123.38 (s, C10), 121.27 (s, C6), 120.13 (s, C5), 118.77 (s, C7), 111.60 (s, C3), 110.24 (s, C8), 106.54 (s, C_6H_4), 101.02 (s, C_6H_4), 94.03 (s, C_6H_4), 46.23 (s, C1), 32.97 (s, C2), 23.20 (s, *C*HMe$_2$), 22.75 (s, *C*H$_3$), 18.72 (s, CH*Me*$_2$).

General Synthesis of [(η^6-arene)Ru{η^3-(*S,S,C′*)-$SC_2B_{10}H_{10}SC'R_2$}] [C′R$_2$ = (COOMe)C═C(COOMe) (9: arene = *p*-cymene (9a), C_6Me_6 (9b)), HC═CPh (10: arene = C_6Me_6 (10b))]. In a typical run **3** (1.0 mmol) and alkynes were dissolved in toluene (15 mL) under argon, and the solution was stirred for 8 h at 110 °C. The blue color of the solution slowly faded to give a yellow solution, suggesting the formation of an adduct. The completion of the reaction was monitored by TLC. The solution was reduced in vacuo to about half its original volume, and some insoluble material was removed by filtration. Addition of hexane to the resulting solution afforded **9** and **10** as a dark yellow precipitate.

Analytical Data for 9a. 9a was prepared from 4.0 mmol (0.48 mL) of dimethyl acetylenedicarboxylate. After recrystallization from toluene, **9a** (0.55 g, 0.94 mmol, 94% yield) was isolated as a yellow solid. Anal. Calcd for $C_{18}H_{30}B_{10}S_2RuO_4$: C, 37.04; H, 5.18. Found: C, 37.12; H, 5.25. IR (KBr, cm^{-1}): ν(B−H) 2582, ν(CO) 2362, ν(C═C) 1631. ^{1}H NMR (300.1 MHz, ppm, $CDCl_3$): 5.63, 5.50 (AA′BB′, 4H, C_6H_4, $J_{Ha-Hb} = 6.0$ Hz, $J_{Ha'-Hb'} = 6.0$ Hz), 3.81 (s, 3H, O*Me*), 3.72 (s, 3H, O*Me*), 2.66 (sp, 1H, C*H*Me$_2$), 2.09 (s, 3H, CH_3), 1.29 (d, 6H, CH*Me*$_2$, $J_{H-H} = 6.6$ Hz). ^{13}C{^{1}H} NMR (75.4 MHz, ppm, $CDCl_3$): 190.95 (s, MeO*C*O), 171.84 (s, MeO*C*O), 157.55 (s, MeOCO*C*═), 123.00 (s, MeOCO*C*═), 99.77 (s, C_6H_4), 95.03 (s, C_6H_4), 89.07 (s, C_6H_4), 88.52 (s, C_6H_4), 53.59 (s, O*Me*), 52.39 (s, O*Me*), 30.99 (s,*C*H$_3$), 22.99 (s, CH*Me*$_2$).

Analytical Data for 9b. 9b was prepared from 4.0 mmol (0.48 mL) of dimethyl acetylenedicarboxylate. After recrystallization from toluene, **9b** (0.48 g, 0.79 mmol, 79% yield) was isolated as a yellow solid. Anal. Calcd for $C_{20}H_{34}B_{10}S_2RuO_4$: C, 39.27; H, 5.60. Found: C, 39.33; H, 5.70. IR (KBr, cm^{-1}): ν(B−H) 2580, ν(CO) 1710, (C═C) 1579. ^{1}H NMR (300.1 MHz, ppm, $CDCl_3$): 3.83 (s, 3H, O*Me*), 3.74 (s, 3H, O*Me*), 2.08 (s, 18H, C_6Me_6). ^{13}C{^{1}H}NMR (75.4 MHz, ppm, $CDCl_3$): 190.84 (s, MeO*C*O), 157.60 (s, MeO*C*O), 145.62 (s, MeOCO*C*═), 123.06 (s, MeOCO*C*═), 99.78 (s, C_6Me_6), 94.96 (s, C_6Me_6), 53.09 (s, O*Me*), 51.27 (s, O*Me*), 15.92 (s, C_6Me_6), 15.65 (s, C_6Me_6).

Analytical Data for 10b. 10b was prepared from 4.0 mmol (0.40 mL) of phenylacetylene. After recrystallization from toluene, **10b** (0.26 g, 0.45 mmol, 45% yield) was isolated as a yellow solid. Anal. Calcd for $C_{22}H_{34}B_{10}S_2Ru$: C, 46.21; H, 5.99. Found: C, 46.28; H, 6.10. IR (KBr, cm^{-1}): ν(B−H) 2600, ν(C═C) 1488, ν(C═C) 1442. ^{1}H NMR (300.1 MHz, ppm, $CDCl_3$): 7.30 (s, 5H, *Ph*), 6.42 (s, 1H, C═C*H*), 1.73 (s, 18H, C_6Me_6). ^{13}C{^{1}H} NMR (75.4 MHz, ppm, $CDCl_3$): 192.05 (s, HC═*C*Ph), 176.64 (s, H*C*═CPh), 127.58 (m, *Ph*), 86.70 (s, C_6Me_6).

Reaction of 3 with Me_3SiCHN_2. A solution of complex **3a** (0.1 g, 0.23 mmol) in toluene (20 mL) was treated with a 2.0 M hexane solution of (trimethylsilyl)diazomethane (0.2 mL, 0.4 mmol) at room temperature for 5 min. The blue color of the solution quickly faded to give a yellow solution. The volatile substances were then removed in vacuo, and the resulting solid was extracted with CH_2Cl_2. Addition of hexane to the concentrated extract gave complex **11a** as yellow-orange crystals. Yield: 0.10 g (0.19 mmol, 83%). Data for **11a**. Anal. Calcd for $C_{16}H_{34}B_{10}S_2RuSi$: C, 36.41; H, 6.49. Found: C, 36.50; H, 6.55. IR (KBr, cm^{-1}): ν(B−H) 2582. ^{1}H NMR (300.1 MHz, ppm, $CDCl_3$): 5.83, 5.73 (AA′BB′, 4H, C_6H_4, $J_{Ha-Hb} = 6.0$ Hz, $J_{Ha'-Hb'} = 6.0$ Hz), 3.53 (s, 1H, Me_3SiCH), 2.54 (sp, 1H, C*H*Me$_2$), 2.22 (s, 3H, CH_3), 1.25 (d, 6H, CH*Me*$_2$, $J_{H-H} = 6.6$ Hz), 0.16 (s, 9H, Si*Me*$_3$). ^{13}C{^{1}H} NMR (75.4 MHz, ppm, $CDCl_3$): 104.47 (s, C_6H_4), 95.52 (s, C_6H_4), 84.90 (s, C_6H_4), 43.88 (s, Me_3SiCH), 32.18 (s, *C*H$_3$), 23.94 (s, CH*Me*$_2$), 0.31 (s, Si*Me*$_3$).

11b. 11b was prepared from 0.21 mmol of **3b**. After flash chromatography on silica gel with hexane/$CHCl_3$ (90:10), **11b** was isolated as an orange solid. Yield: 0.11 g (0.19 mmol, 90%). Data for **11b**. Anal. Calcd for $C_{18}H_{38}B_{10}S_2RuSi$: C, 38.89; H, 6.89. Found: C, 38.95; H, 6.94. IR (KBr, cm^{-1}): ν(B−H) 2596, ν(B−H) 2568. ^{1}H NMR (300.1 MHz, ppm, $CDCl_3$): 3.51 (s, 1H, Me_3SiCH), 2.15 (s, 18H, C_6Me_6), 0.18 (s, 9H, Si*Me*$_3$). ^{13}C{^{1}H} NMR (75.4 MHz, ppm, $CDCl_3$): 94.69 (s, C_6Me_6), 87.53 (s, C_6Me_6), 22.78 (s, Me_3SiCH), 17.11 (s, C_6Me_6), 16.63 (s, C_6Me_6), −0.05 (s, Si*Me*$_3$).

X-ray Crystallography. Suitable crystals of **4b**, **5b**, **8b**, and **11b** were obtained by slow diffusion of hexane into a methylene chloride solution of the complexes at room temperature and were mounted on a glass fiber. Crystal data and experimental details are given in Table 1. The data sets for **4b**, **5b**, **8b**, and **11b** were collected on an Enraf CAD4 automated diffractometer. Mo Kα radiation ($\lambda = 0.7107$ Å) was used for all structures. Each structure was solved by the application of direct methods using the SHELXS-96 program[25a] and least-squares refinement using SHELXL-97.[25b] All non-hydrogen atoms in compounds **4b**, **5b**, **8b**, and **11b** were refined anisotropically. All other hydrogen atoms were included in calculated positions.

Acknowledgment. The support of this research by a Korea Science & Engineering Foundation Grant (R01-2000-00050) is gratefully acknowledged. This work was also supported by the Brain Korea 21 project in 2000.

Supporting Information Available: Crystallographic data (excluding structure factors) for the structures (**4b**, **5b**, **8b**, and **11b**) and CV data for complex **8a** reported in this paper. This material is available free of charge via the Internet at http://pubs.acs.org.

OM020259L

(25) (a) Sheldrick, G. M. *Acta Crystallogr. A* **1990**, *46*, 467. (b) Sheldrick, G. M. *SHELXL*, Program for Crystal Structure Refinement; University of Göttinen, 1997.